Effect of Non-Integer Scaling on the Recovery of Data-bearing Marks

Robert Ulichney[1], Yufang Sun[2], Matthew Gaubatz[3], Stephen Pollard[4]
HP, Inc., [1]Stow, MA USA, [2]Indianapolis, IN, USA, [3]Seattle, WA, USA, [4]Bristol, UK

Abstract

The spatial quantization imparted by printed pixels becomes significant when printing finely detailed bitonal images such as data-bearing halftones. This paper explores the consequences non-integer scaling has on data recovery error from such data-bearing marks. We verify that different printer manufacturers use nearest-neighbor scaling, and conducted hundreds of print and mobile camera capture measurements to quantify data recovery errors as a function of printed pixel replication factor. We tested the effects of multiple payloads represented by several data-bearing images, printed on a variety of printers, and captured at different camera distances. The analog print–and-capture experiments are compared with digital simulations, using several error measures. The results support a surprising conclusion: there is no significant advantage in forcing printed pixel replication to be an integer.

Introduction

Embedding data in and recovering data from hardcopy are key steps in a variety of information-rich applications. As the resolution and close-focus ability of mobile cameras increase, the marks for embedding data in hard copy continue to decrease in size. Embedding schemes such as QR or data matrix codes involve represented symbols with relatively large binary squares, and are robust to scaling effects. Higher density solutions such as data-bearing halftones [1][2] can require more careful registration for accurate decoding. In the case of stegatones [3], the focus of this paper, data is represented by single-pixel shifts of halftone clustered dots. A convenient assumption that helps promote robust recovery of these designs is that a physical rendering from input pixels to device pixels must be scaled by an integer, such that single pixel perturbations translate cleanly into the rendered image space.

There are, however, situations where this integer relationship cannot be guaranteed. An important case is that when a document is prepared with a fixed size mark, but the printer is not yet known. 400 dpi data-bearing halftones have yielded a good blend of payload density and recoverability. While a document with such a mark will render beautifully on a 1200dpi printer (with a replication factor of 3X), a potential problem arises with a 600dpi printer. The printed pixel replication factor will be 1.5, meaning some input pixels are represented by 2x2 device pixels and some are represented by a single (1x1) pixel. Changing the image size will also introduce non-integer replication factors. For fine details, the effects of non-integer scaling can be significant, and in fact, a halftone strategy that attempts to create imagery suitable for a set of different scales has been proposed [4].

Consider the example of scaling a one-pixel wide line as shown in Figure 1(a) by a factor of 1.6. Nearest-neighbor scaling will render the line as shown in (b). The uniform input line is now composed of segments with 4 different shapes. Bilinear scaling produces the gray scale version in (c) which is visually more uniform but cannot be rendered on most printers which are inherently bitonal.

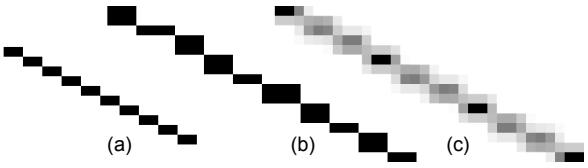

Figure 1. *Scaling a one-pixel wide line by 1.6x. (a) Input, (b) Nearest-neighbor scaling, (c) Bilinear scaling.*

The generation of a stegatone is illustrated in Figure 2. A continuous-tone input image (a) is halftoned (b) using a classical 45-degree clustered-dot screen. A data payload in embedded by single-pixel shifting the halftone clusters to produce the stegatone in (c). For this particular 200x200 pixel image the payload capacity is 1488 raw bits, with an error-corrected capacity of 376 bits. Nearest-neighbor scaling the stegatone by a factor of 1.6 produces the binary image in (d). A small area from the left side of the stegatone is enlarged in Figure 3. A region form the input image is shown in (a) with uniform 2x2 pixel clusters. The 1.6x scaled version of the same area in (b) reveals clusters of size 3x3, 4x4, 3x4, and 4x3 pixels.

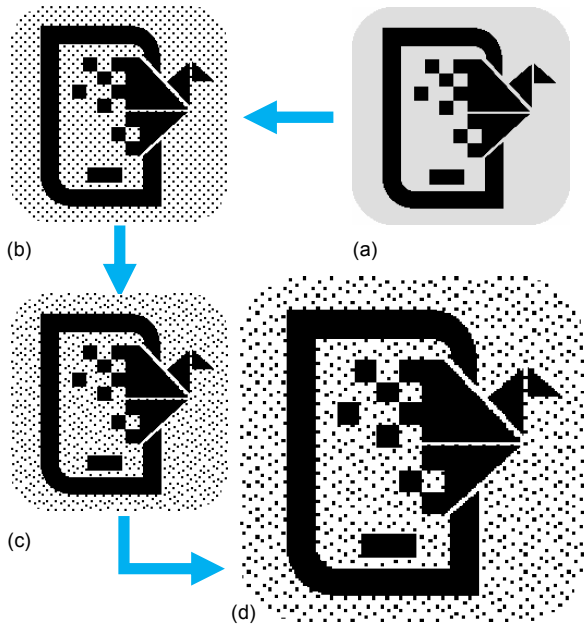

Figure 2. *Stegatone generation and printing. (a) Gray scale input image, (b) Clustered-dot halftone, (c) Stegatone, and (d) Scaled by 1.6x when printed.*

While the impact of image scaling on quality assessment [5][6], watermarking [7], image matching [8] and QR code detection [9] schemes have been previously studied, the focus in most cases has been on digitally scaled images, as opposed to content scaled, (physically) rendered content captured with an imaging device. The multiscale Viola-Jones object detection scheme was applied to a fast QR code detection problem and found to reveal encouraging results on actual (streamed) mobile imagery [9]. Compounding the problem, the art of scaling binary images for binary display [10][11] can be more challenging than when using continuous-tone images; efforts have often focused on the visual appearance rather than detectability, or recoverability.

Though much research has been done analyzing the effects of scaling imagery on various functional measurements based on that imagery, the effects of up-scaling binary halftone-based data representations are less well understood. How does this effect alignment and data recovery? Do some replication factors, such as perfect integers, perform better than others? How does capture resolution interact with printed pixel replication? We address these questions in this work.

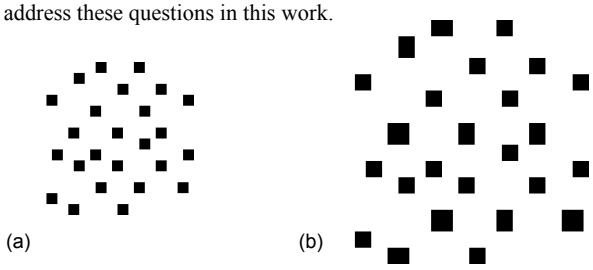

Figure 3. *Nearest-neighbor scaling of an array of 2x2 clusters by 1.6x.*

Assessing Printer Scaling

To measure the data recovery error rates of a printed stegatone after upscaling by non-integer factors we used 4 laser printers of different manufactures, two with a resolution of 600 dpi and two with a resolution of 1200 dpi. We will anonymously identify the printers as A600, B600, C1200 and D1200. To ascertain how scaling is performed on these printers we used the test pattern shown in Figure 4. It is 240x240 pixels where every row and every column has exactly one single-pixel wide black line segment. We printed copies of this pattern scaled in small increments form 1.0 to 2.0 in the native resolution (600 or 1200 dpi) on each of the 4 printers. This allowed us to observe exactly which rows and columns were pixel replicated.

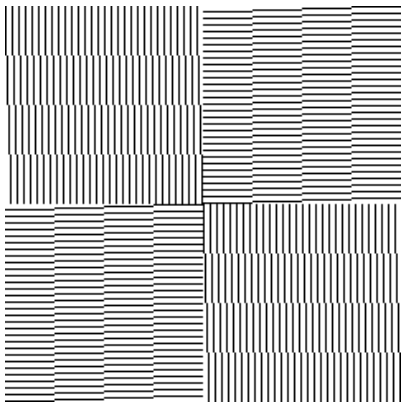

Figure 4. *Digital pattern to test nature of scaling.*

The results revealed that all four printers were indeed scaling by nearest-neighbor. One scale factor that makes this effect clearly evident is 1.5x with scans of the resulting prints in Figure 5. The 1200 dpi prints are half the size of the 600 dpi prints, but are shown at the same size for the purpose of illustration. A 1.5 scale factor will replicate every other pixel both horizontally and vertically. As every other line is doubled in thickness a resonant pattern is seen. The patterns for the four printers are identical except for a one-pixel phase difference in the horizontal direction.

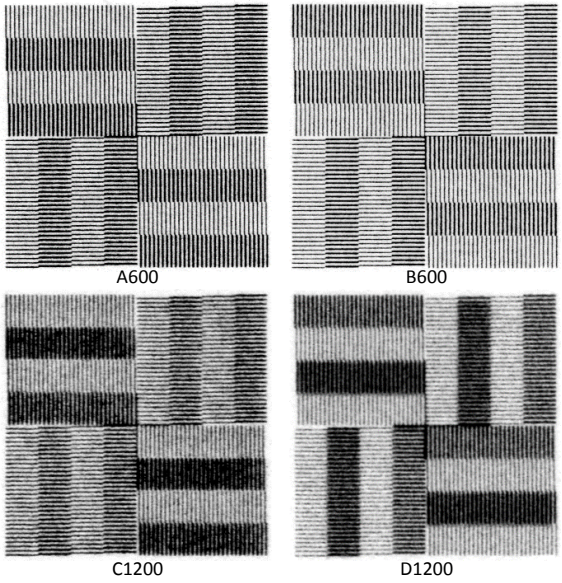

Figure 5. *Results of scaling by 1.5x. Output from 4 different printers.*

As another example and evidence of nearest-neighbor scaling, the prints for scale factor 1.6 are shown in Figure 6. For this scale factor there are 8 output pixels for every 5 input pixels, so 3 lines are doubled for every 5 in the pattern. This effect is seen for all four printers with identical patterns, except for a one-pixel phase shift in the vertical direction.

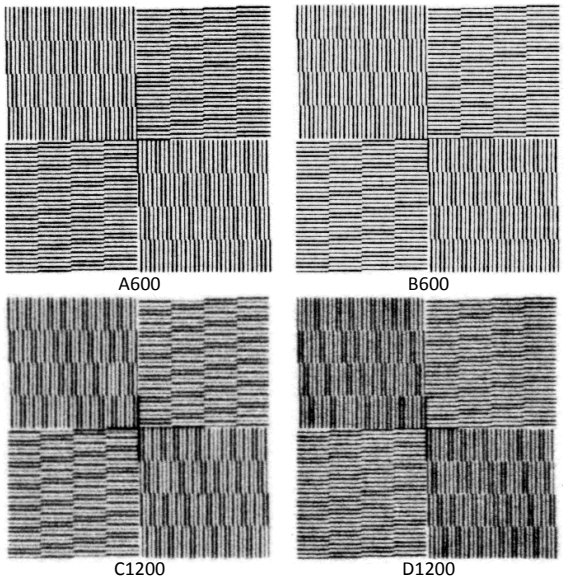

Figure 6. *Results of scaling by 1.6x. Output from 4 different printers.*

Error Rates from Mobile Capture

Starting with the A600 printer, we printed a set of scaled versions of the "bird" stegatone from Figure 2(c). In terms of the native 600 dpi resolution of the printer, we scaled the stegatone in terms of "printed pixel replication" factors. A printed pixel replication factor of 1.0 means there is a one-to-one relationship between input pixels and printed pixels. For this test we used printed pixel replication factors of 1.0 to 3.0 in steps of 0.1. Each of these 21 printed scaled stegatone was then captured with a mobile phone camera using video mode at a mechanically fixed distance of 8.5 cm from the printed page. At this distance the capture sampling rate was measured to be 672 dpi. A frame from the video was then processed using a recovery algorithm that aligns the image, then detects the shift of each halftone cluster to determine the raw data bits. Those bits were compared to the original data bits, and the percent of incorrect bits were recorded as the "raw bit error rate percent".

This entire procedure was repeated for five versions of the same stegatone each with a different data payload. The results of the measured raw bit error rates are plotted in Figure 7 for the 5 payloads. On the top of the plot the x-axis is labeled with the "effective print resolution," which represents the native print resolution, 600 dpi, scaled by the printed pixel replication factor. The average of the results from the stegatones with the 5 payloads is shown as the red curve in Figure 8. Also plotted in this figure is the average of the error correction coding (ECC) enhanced payload in blue, determined by using ECC applied to the payload to mitigate errors in the recovered raw bits.

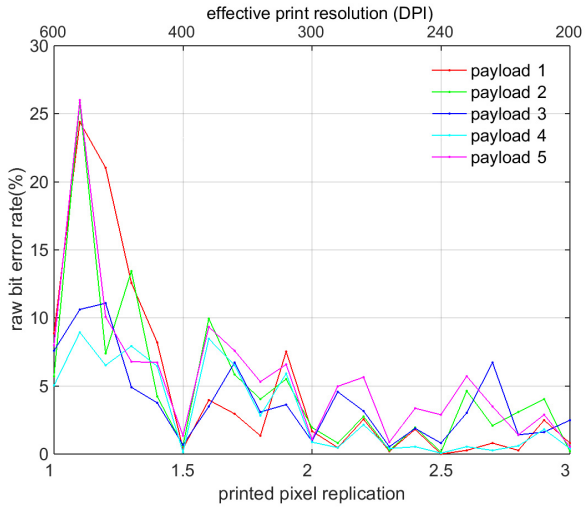

Figure 7. *Raw bit error rate for printer A600, captured at 8.5 cm for 5 different payloads.*

This entire process was then repeated with the mobile phone camera at two other distances: 11.5 cm and 14.3 cm. These distances were chosen to correspond to measured video capture resolutions of 500 and 400 dpi, respectively. The purpose of these changes was to observe if printed pixel replication factor, or equivalently effective print resolution, interacted in some periodic or otherwise notable way with capture resolution. These results are shown in Figure 9. To our surprise capture resolution had no effect. The shape of the curves were the same, with the expected slight increase in error as the capture distance increased.

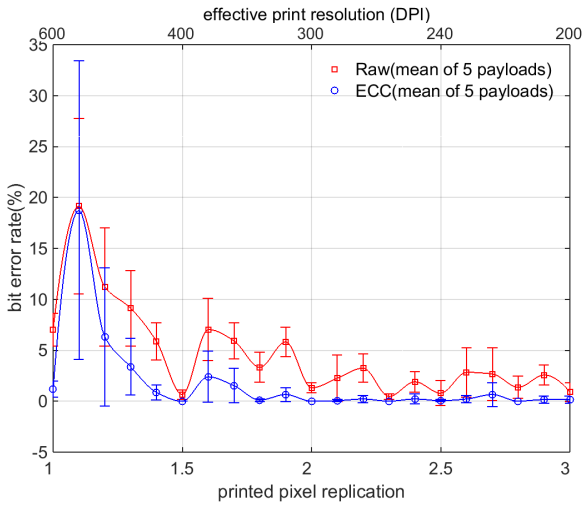

Figure 8. *Average raw bit error rate and ECC error rate for printer A600, captured at 8.5 cm.*

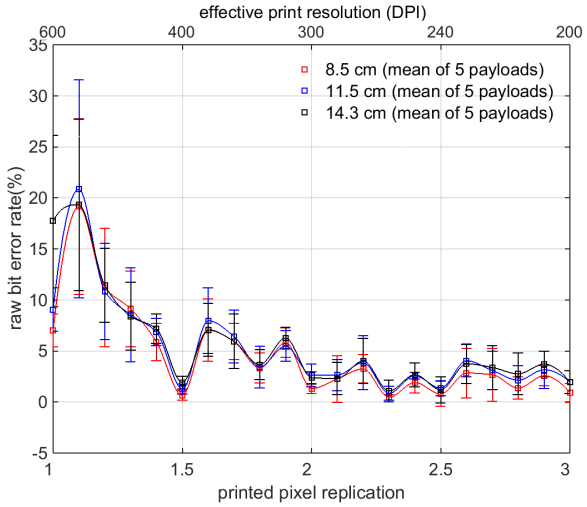

Figure 9. *Average raw bit error rate for printer A600 across 5 payloads at video capture distances of 8.5, 11.5, and 14.3 cm.*

All of these procedures were then applied with the other 600 dpi printer (B600). To summarize, there are 21 printed pixel replication factors (or scales), 5 payloads, and 3 capture distances for another 315 experiments. Those results are plotted in Figure 10. Like the A600 printer, it too showed high correlation between results obtained at different capture distances. Both printers showed a sharp increase in error at printed pixel replication factor of 1.1. However, at 1.5 printer A600 showed a clear decrease in error while printer B600 showed an error increase.

For the first 1200 dpi printer, C1200, we needed to adjust the range of the printed pixel replication factors, due to the following. Because of the higher print resolution, we started at a pixel replication factor of 1.5, which has an effective print resolution of 800 dpi. This resolution is already higher than our highest capture resolution of 672 dpi when the camera is 8.5 cm from the print. For this printer we extend the printed pixel replication factors a bit further out to 6.0. The results for the measured raw bit error rates are shown in Figure 11.

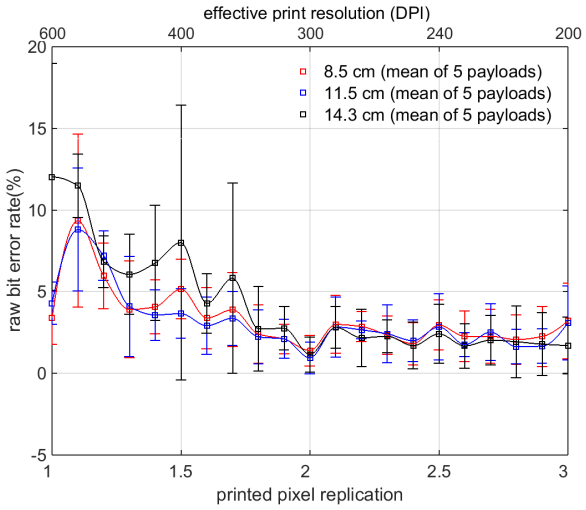

Figure 10. *Average raw bit error rate for printer B600 across 5 payloads at video capture distances of 8.5, 11.5, and 14.3 cm.*

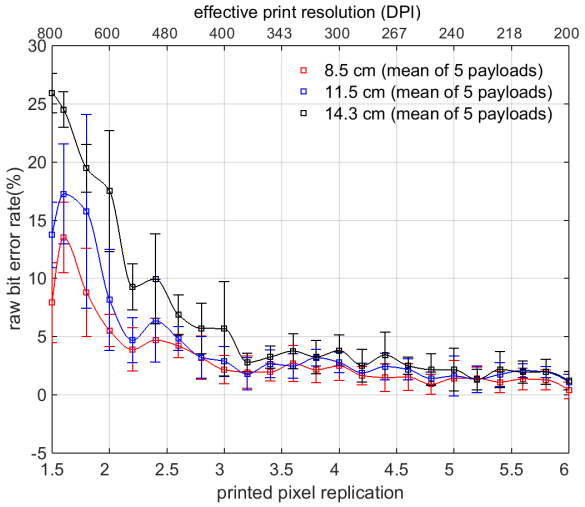

Figure 11. *Average raw bit error rate for printer C1200 across 5 payloads at video capture distances of 8.5, 11.5, and 14.3 cm.*

The error rate above printed pixel replication factor of 4.0 appears to reach steady state; for this reason there is no need for further testing above that factor. Accordingly, the range of printed pixel replication factors for the other 1200 dpi printer (D1200), was set from 1.5 to 4.0. Its results are shown in Figure 12. While both 1200 dpi printers show increased errors at the high effective print resolutions, they, like the 600 dpi printers, show no real preference for integer printed pixel replication factors, or any interaction with capture resolution.

Another metric we measured was mean-squared error (MSE). The reference is the unscaled bitonal stegatone. This image is compared with the up-scaled version that is printed, video captured, tone-scale adjusted to cancel illumination effects, then down-scaled to the same digital size as the reference using a bilinear method. These measurements were applied to the captures using the A600 printer at the three distances and 5 payloads, and plotted in Figure 13. Comparing the shape of this plot to the data shown in Figure 9 reveals some differences. The MSE shows more separation as capture distance increases, and a more steady decrease as printed pixel replication factor increases. But again, there is no real preference for integer pixel replication factors over non-integer factors.

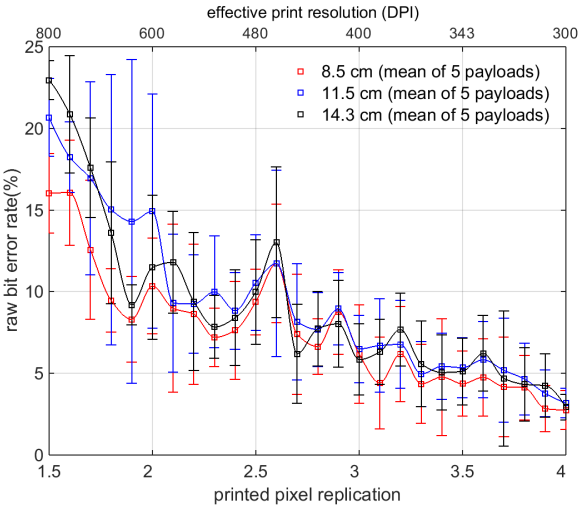

Figure 12. *Average raw bit error rate for printer D1200 across 5 payloads at video capture distances of 8.5, 11.5, and 14.3 cm.*

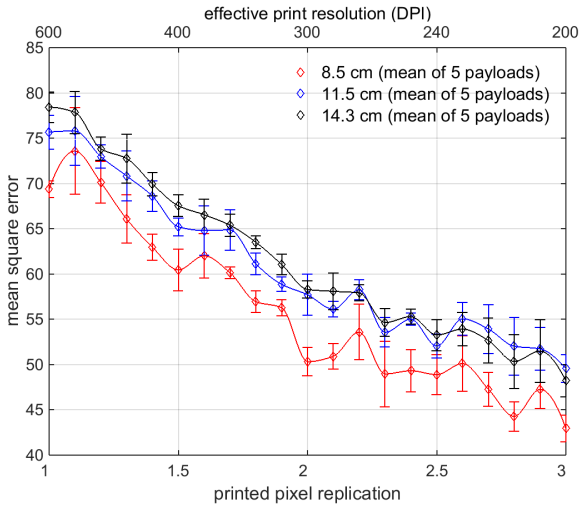

Figure 13. *Average mean square error for printer A600 across 5 payloads at video capture distances of 8.5, 11.5, and 14.3 cm.*

To analyze the effect of different stegatone source images, we included 3 additional images shown in Figure 14, two portraits with varying size dot clusters, and a short piece of (halftoned) text. Along with the original bird stegatone from Figure 2(b), we printed scaled versions of the four stegatones for each of 5 payloads and printed them on the A600 printer. These images were all captured at 8.5 cm. The raw bit error rates are plotted in Figure 15. While all four images show similar performance, the "Stega" text image suffered higher errors at the lowest pixel replication factors; unlike the other prints, this design is dominated by shadow cells (the white dots surrounded by black) and printer dot gain makes them harder to locate.

The average raw error rate for all four images in Figure 15 is plotted as the red curve in Figure 16. It follows the shape of bird-only curve in Figure 9. Figure 16 also shows the average ECC error in blue. An additional metric is also plotted in that figure: "Pixel error rate" is the percent of binary pixels that are different between the original source stegatone and a size-

reduced version of the captured image. Bilinear scaling is used to match the size of the captured image to the original image. The image is then binarized using an adaptive threshold according to [12]. The average pixel error rate is plotted in black in Figure 16. Interestingly, it is more linear than the recovered bit error rate.

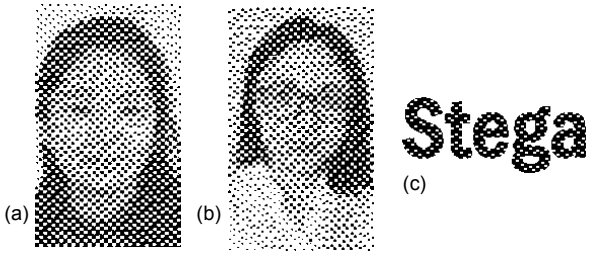

Figure 14. *Three additional stegatone images to test. (a) Portrait 1, (b) Portrait 2, and (c) The text "Stega".*

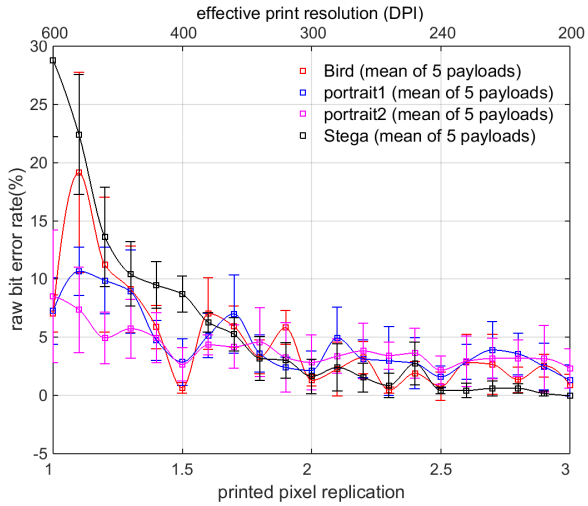

Figure 15. *Average raw bit error rate for 4 different source images for printer A600 across 5 payloads at a video capture distance of 8.5 cm.*

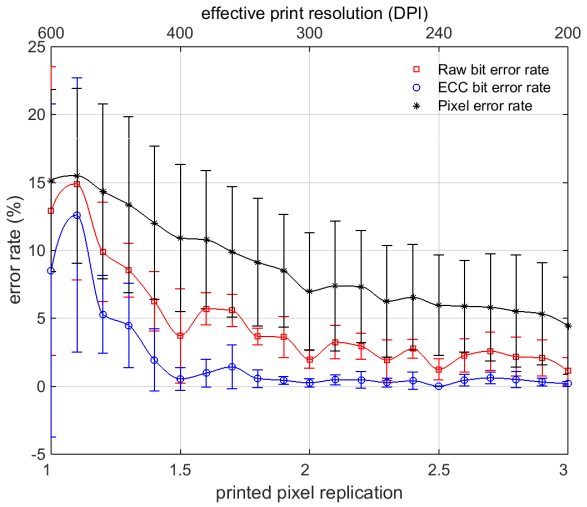

Figure 16. *Average raw bit error rate, ECC error rate, and pixel error rate for 4 different source images for printer A600 across 5 payloads at a video capture distance of 8.5 cm.*

All-Digital Simulation

To examine the analogue degradations due to printing and camera capture from another perspective, it is instructive to examine the effect of scaling by means of an all-digital simulation. For this experiment we use bird stegatone from Figure 2(c) and scaled it to simulate a "digital printer". We used nearest-neighbor scaling to match what our four printers actually do. Also, to simulate a printer that could print true continuous tone, we scaled the stegatone using a bilinear method. For both cases the scaled input was used as the "captured" image and processed in the same way as we processed the camera captured versions of printed hard copy.

The resulting raw bit error rate averaged over 10 different data payloads is plotted in Figure 17. The red curve represents the result for scaling the input image using nearest-neighbor scaling, and the blue curve is the result for using bilinear scaling. The nearest-neighbor curve resembles the shape in Figure 9, but with a much lower amplitude (as we would expect for an all-digital experiment). The simulated bilinear scaled experiment resulted in very low raw bit error. This is due to the fact that the recovery system detects clustered dot shifts by finding centroids of the captured gray scale blobs; bilinear scaled input will preserve the center position better than a hard binary threshold of pixels. Somewhat surprisingly the bilinear error curve is nearly uniform across the range of pixel replication factors.

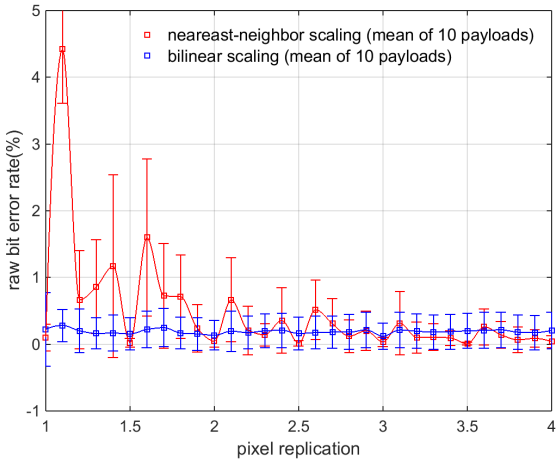

Figure 17. *Average raw bit error rate for the bird image with 10 different payloads for a digitally simulated printer that pixel replicates by nearest-neighbor and bilinear scaling.*

We measured MSE in the same way in our digital simulations as was done in Figure 13. The results for both nearest-neighbor and bilinear scaling is shown in Figure 18. In this case bilinear scaling suffered generally higher MSE. While bilinear scaling preserves the center positions of dot clusters better than nearest-neighbor, it differs more on a pixel-by-pixel basis with the bitonal sources image. Finally, we measured pixel error using the process described for Figure 16, except the captured image is a digitally scaled image. The results are plotted in Figure 19. These results are very similar to those for the simulated raw bit error but for different reasons. Like MSE pixel error is a pixel-by pixel measure, however the adaptive binarization of the down-scaled image forces a more accurate match with the binary source image.

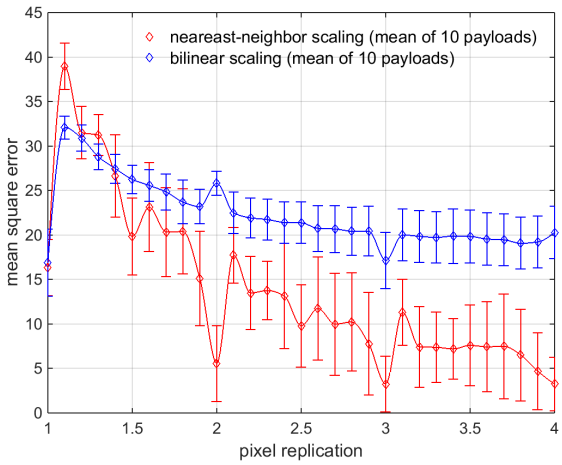

Figure 18. *Average MSE for the bird image with 10 different payloads for a digitally simulated printer that pixel replicates by nearest-neighbor and bilinear scaling.*

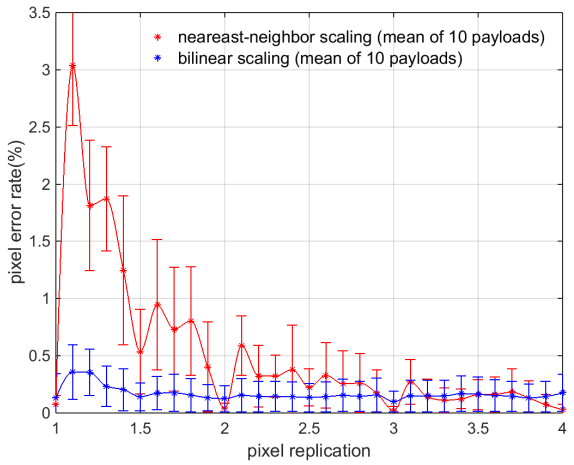

Figure 19. *Average pixel error rate for the bird image with 10 different payloads for a digitally simulated printer that pixel replicates by nearest-neighbor and bilinear scaling.*

Concluding Remarks

This work revealed some surprises and validated some assumptions. Our measurements verified that among all the printers we tested, binary raster images are enlarged by nearest-neighbor scaling. Our experiments showed that sampling resolution, determined by the distance the camera is from the print, does not alter the performance of recovery other than the expected uniform increase in error across pixel replication factors; there is no beat frequency effect between sample frequency and printed pixel frequency.

In our all-digital experiments an advantage for perfect integer pixel replication factors was shown for MSE (Figure 18) and pixel error (Figure 19). But, where it really matters, for alignment and data recovery the experiments indicate that there is no significant advantage in forcing printed pixel replication to be an integer. This result represents a distinct advantage for the management of distributed rendering environments where the precise scale between document preparation and device resolutions cannot be controlled.

References

[1] O. Bulan, V. Monga, G. Sharma, and B. Oztan, " Data embedding inhardcopy images via halftone-dot orientation modulation," in *Proc. SPIE Int. Conf. Security, Steganography, and Watermarking of Multimedia Contents X*, vol. 6819, pp. 68190C-1-12, Jan. 2008.

[2] N. Damera-Venkata, J. Yen, V. Monga, B. Evans, "Hardcopy Image Barcodes Via Block-Error Diffusion", *IEEE Transactions On Image Processing*, Vol. 14, No. 12, pp. 1977-1989, 2005.

[3] R. Ulichney, M. Gaubatz, and S. Simske, "Encoding Information in Clustered-Dot Halftones", *IS&T NIP26 (26th Int. Conf. on Digital Printing Technologies), Austin, TX*, 602-605, Sep 2010.

[4] Y.-H. Fung and Y.-H. Chan, "Embedding halftones of different resolutions in a full-scale halftone," *IEEE Signal Processing Letters*, Vol. 13, No. 3, pp. 153-156, 2006.

[5] Prasantha H. S., Shashidhara H. L. and Balasubramanya Murthy K. N., "Image scaling comparison using universal quality index," *Proc. IEEE Int. Conf. on Advances in Computing, Control, and Telecommunication Technologies*, pp. 859-863, 2009.

[6] M. Gaubatz and S. Hemami, "On the nearly scale-independent rank behavior of image quality metrics," *Proc. IEEE Int. Conf. on Image Processing (ICIP)*, pp. 701-704, 2008.

[7] C.-Y. Lin, M. Wu, J. A. Bloom, I. J. Cox, M. L. Miller and Y. M. Lui, "Rotation, scale and translation resilient watermarking for images," *IEEE Transactions on Image Processing*, Vol. 10, No. 5, pp. 767-862, May 2001.

[8] S. Todorovic and N. Ahuja, "Scale-invariant region-based hierarchical image matching," *Proc. IEEE. Int. Conf. on Pattern Recognition (ICPR)*, pp. 1-5, 2008.

[9] L. Belussi and N. Hirata, "Fast QR code detection in arbitrarily acquired images," *24th SIBGRAPI Conference on Graphics, Patterns and Images*, pp. 281-288, 2011.

[10] E. Danahy, S. Agaian and K. Panetta, "Algorithms for the resizing of binary and grayscale images using a logical transform", *Proceedings of SPIE,* vol. 6497, 2007.

[11] R. Ambareesh; B. Nath, "Binary image scaling for miniature monochrome embedded displays using mathematical discretization", *IEEE Int. Advance Computing Conference (IACC*), pp 754-759, 2015.

[12] N. Otsu, "A threshold selection method from gray-level histogram", *IEEE Transactions on Systems, Man, And Cybernetics*, Vol. SMC-9, No. 1, 1979.

Author Biography

Robert Ulichney is a Distinguished Technologist with HP Labs focusing on systems for high capacity data embedding, and structures for variable density 3D printing. He received a Ph.D. from MIT in electrical engineering and computer science. Before joining HP he was with Digital Equipment Corp for several years then with Compaq's Cambridge Research Lab. His publications are available at ulichney.com.